Journal of Architectural Research and Development, 2024, Volume 8, Issue 3
http://ojs.bbwpublisher.com/index.php/JARD
Online ISSN: 2208-3537
Print ISSN: 2208-3529

Analysis of Bonding Properties of Corroded Reinforcement Concrete

Liang Fang*, Yingzhuo Liu

College of Water Resources & Civil Engineering, Hunan Agricultural University, Changsha 410128, Hunan Province, China

Corresponding author: Liang Fang, fangliang@hunau.edu.cn

Abstract: In order to investigate the degradation of bonding properties between corroded steel bars and concrete, this study employs the half-beam method to conduct bond-slip tests between corroded steel bars and concrete after impressed-current accelerated corrosion of the steel bars in concrete. The effects of steel corrosion rate, steel bar diameter, steel bar strength grade, and concrete strength grade on the bonding properties between concrete and corroded steel bars were analyzed. The influence of different corrosion rates on specimens' bonding strength and bond-slip curves was determined, and a constitutive relationship for bond-slip between corroded steel bars and concrete was proposed. The results indicate that the ultimate bonding strength of corroded reinforced concrete specimens decreases with increasing corrosion rate. Additionally, an increase in corrosive crack width leads to a linear decrease in bonding strength. Evaluating the decline in adhesive properties through rust expansion crack width in engineering applications is feasible. Furthermore, a bond-slip constitutive relationship between corroded steel bars and concrete was established using relative bond stress and relative slip values, which aligned well with the experimental findings.

Keywords: Corrosion; Reinforced concrete; Bonding property; Constitutive relation

Online publication: June 17, 2024

1. Introduction

Steel corrosion is one of the main reasons for the reduction of the service life of reinforced concrete components. Corrosion of steel bars will lead to cracking of components, decrease of effective cross-sectional area, and decrease of bonding performance between steel bars and concrete [1-3]. Further investigation of the degradation pattern in the bonding performance between corroded steel and concrete enables us to more precisely assess the residual load-bearing capacity of the component, facilitating targeted maintenance and reinforcement measures.

Since the 1950s, researchers both domestically and internationally have conducted extensive and long-term studies on the bond-slip performance between corroded steel and concrete. A large number of experimental studies have demonstrated that the bonding strength between steel bars and concrete exhibits an initial increase followed by a decrease as the corrosion rate of the steel bars increases [4-9]. Eligehausen *et al.* [10,11] first proposed

a four-segment adhesive slip constitutive relationship model based on experimental research, which is adopted by the European Model Specification. The five-stage bond-slip constitutive model proposed by Xu *et al.* [12] through experimental research is mainly adopted in the design code of concrete structures in China. Somayaji *et al.* [13], Zhao *et al.* [14], and Wu *et al.* [15] respectively used theoretical analysis combined with experimental methods to derive the bond-slip constitutive model. Due to the elimination of abrupt changes in the rising and falling sections of multi-segment τ-*s* curves, this type of model is more suitable for finite element analysis. In addition, Nilson [16] used the strain of concrete near the bonding interface to replace the strain of interface concrete and derived a τ-*s* constitutive relationship that varies with position. Yuan *et al.* [9,17] concluded that the bond-slip constitutive curve of corroded reinforced concrete components was basically similar to that of non-corroded ones after conducting the eccentric pull-out test on corroded steel members constrained by stirrup, and also established a five-stage bond-slip constitutive relationship model. Zhang *et al.* [18] established a multi-stage bond-slip constitutive model with the width of corrosive crack width as the control index through the half-beam test. The research results of Yuan *et al.* [9,17] and Zhang et al. [18] both believed that the ratio of residual bonding strength to peak bonding strength of corroded steel components is not affected by the degree of corrosion. On the contrary, the research results of Kivell *et al.* [19] suggest that this ratio changes with different corrosion rates of steel bars. Kivell *et al.* [19] believed that the peak slip amount corresponding to the peak bonding strength remained unchanged, while Yuan *et al.* [9,17] pointed out that the peak slip amount decreased with the increase in corrosion rate. The research findings of Mangat *et al.* [8] indicate that the corrosion rate exceeds 1%, and there is a positive correlation between the corrosion rate and the peak slip amount.

In summary, the service environment of corroded steel bars and concrete is complex, and the coupling effect of many factors is obvious, so the research on its bonding properties has not obtained a unified result. Therefore, further research on the bond-slip constitutive relationship of specimens after steel corrosion has theoretical significance and practical value for evaluating the durability of concrete structures. In this study, the degradation of bonding properties between corroded steel bars and concrete was tested by the half-beam method. The influence of corrosion degree, concrete strength, steel bar strength, and diameter on the degradation of bonding performance was considered. The failure mode of the specimen, the degradation law of bonding strength, and the bond-slip constitutive relationship between corroded steel bars and concrete were analyzed.

2. Experimental design

2.1. Accelerated corrosion test

A total of 16 reinforced concrete slabs were made to accelerate the corrosion of steel bars in concrete. The parameters of the reinforced concrete slab are shown in **Table 1**. The design and manufacture are shown in **Figure 1**. The material strength is shown in **Tables 2** & **3**. The accelerated corrosion test process is described in detail in reference [20].

Table 1. Specimen code and basic parameters

Specimen code	Concrete strength grade	Steel bars strength grade	Diameter of steel bar (mm)	Expected corrosion rate (%)
X1-1C/L/M/H	C40	HRB400	12	0/5%/10%/15%
X1-2C/L/M/H	C40	HRB500E	14	0/5%/10%/15%
X2-1C/L/M/H	C50	HRB400	12	0/5%/10%/15%
X2-2C/L/M/H	C50	HRB500E	14	0/5%/10%/15%

Note: The corrosion rate is the average mass-loss rate of steel bars.

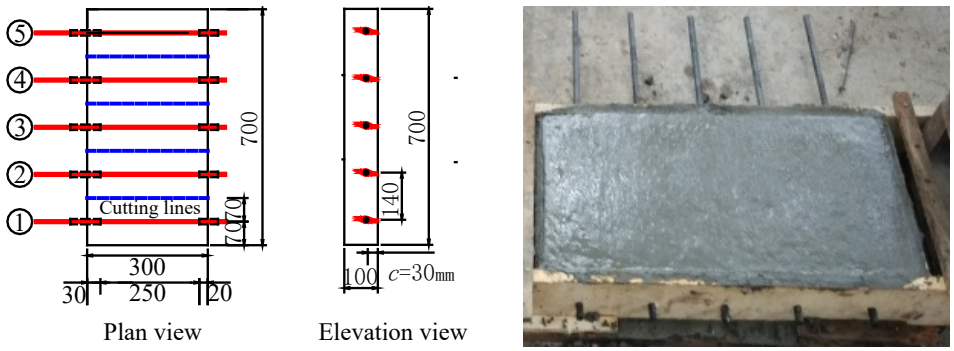

Figure 1. Test specimen (Unit: mm)

Table 2. Compressive and tensile strength of concrete

Concrete grades	C40	C50
Cubic compressive strength (MPa)	46.8	52.8
Split tensile strength (MPa)	3.185	4.543

Table 3. Mechanical property of steel bars

Steel bar's strength grades	Diameter (mm)	Yield strength (MPa)	Ultimate tensile strength (MPa)	Elongation (%)
HRB400	12	487.3	619.4	22.73
HRB500E	14	563.0	726.6	25.53

2.2. Specimen for testing bonding performance

After the accelerated corrosion test, the slab was cut into 5 pieces according to the lines shown in **Figure 1**, of which blocks 3–5 were used for testing the bonding performance between steel bars and concrete. The cut specimen is shown in **Figure 2**.

Figure 2. Specimen for testing bonding performance

The corrosive cracks of the bonding performance specimens mainly appeared at the corresponding positions of the steel bars at the bottom (**Figure 3**). The cut specimens numbered 3 and 4 were located in the middle of the slab, with only one corrosive crack at the bottom (**Figure 4** (a)). A small number of cut specimens numbered 5 had cracks on the side due to being located at the edge of the slab, except for the corrosive crack at the bottom (**Figure 4** (b)).

Figure 3. Photo of corrosive crack of specimen

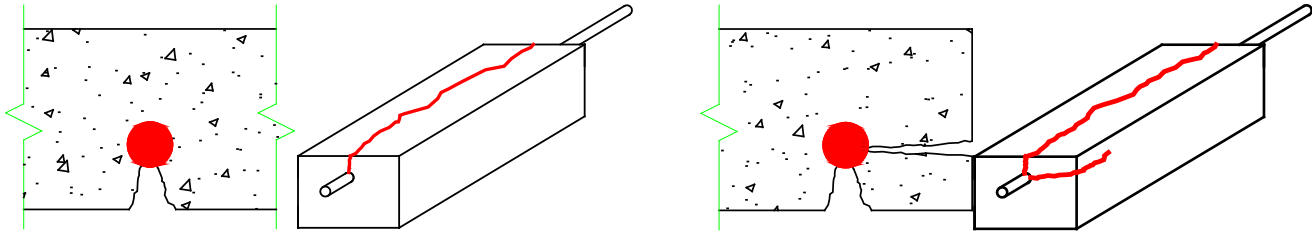

(a) No. 3 and No. 4 (b) No. 5

Figure 4. Types of corrosive cracks of specimens

2.3. Bond-slip test

In this study, the half-beam test method was used to study the bonding performance between steel bars and concrete. The test loading scheme and test conditions are shown in **Figure 5**. By adding steel rollers to the drawing device, the eccentric tension of longitudinal reinforcement in the actual bending member is simulated. There are hard rubber strips between the steel roller and the specimen, to prevent premature local pressure damage at the contact position. The WAW-600 D electro-hydraulic servo universal testing machine was used to load. The loading scheme was controlled by displacement, and the loading speed was 0.5 mm/min. Two displacement meters were set up at the free end of the specimen. The tensile force *N* of the steel bar and the displacement of the steel bar and concrete at the free end of the specimen were recorded during the test. The test was completed when the specimen had a splitting failure, bending-shear failure, bond slip failure, or slip amount exceeding 2 mm. The corrosion rate of steel bars was determined through the mass loss rate. After the bond-slip test, the corroded steel bars were taken out for pickling, drying, weighing, and calculating the corrosion rate.

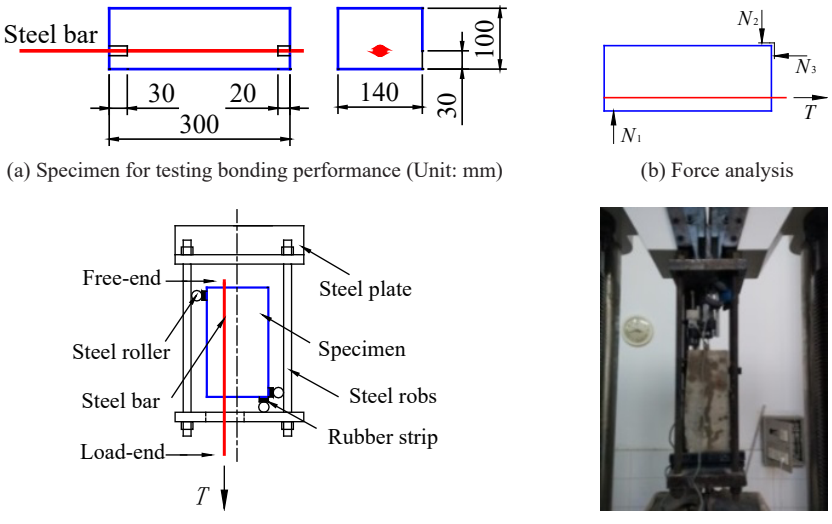

(a) Specimen for testing bonding performance (Unit: mm) (b) Force analysis

(c) Loading scheme (d) On-site photo

Figure 5. Half-beam method

3. Results

Through this half-beam test, it is observed that the failure modes of the specimens were bending shear failure, splitting failure, local compression failure, and steel bar breaking (**Figure 6**). Due to the large bond length of the specimen, no typical slip failure was observed in this test.

When the corrosion rate was low and the width of the corrosive crack was less, the specimen appeared bending-shear cracks similar to the component in bending. During the loading process, the vertical crack developed at bearing No. 1, and then the vertical crack penetrated the protective layer of the specimen and connected with the main crack developing along the longitudinal steel bar. When the specimen failed, concrete near bearings No. 2 and No. 3 was compressed and damaged (**Figure 7**). The concrete on the failure surface of a small number of specimens showed the phenomenon of scraping, that is, the steel bars produced a certain amount of sliding, and the ribs were filled with crushed concrete powder. When the corrosion rate was high and the corrosive crack width was large, the specimen presented a splitting failure of the protective layer along the corrosive crack. The concrete of specimens might be split into 3–4 parts. The concrete on the splitting surface after the failure of the specimen retained clear traces of steel ribs, and there was a small amount of crushed concrete powder between the ribs (**Figure 8**). The specimen N1-2L5 with the concrete strength grade of C40 experienced splitting failure accompanied by local compression failure of the concrete near the bearings (**Figure 9**). The specimen N2-1M3 with the strength grade of steel bar HRB400 showed the steel bar breaking (**Figure 10**). However, specimens N1-1H4 and N1-1H5 with higher corrosion rates were damaged due to excessive expansion of the corrosive cracks. The test results are shown in **Table 4**.

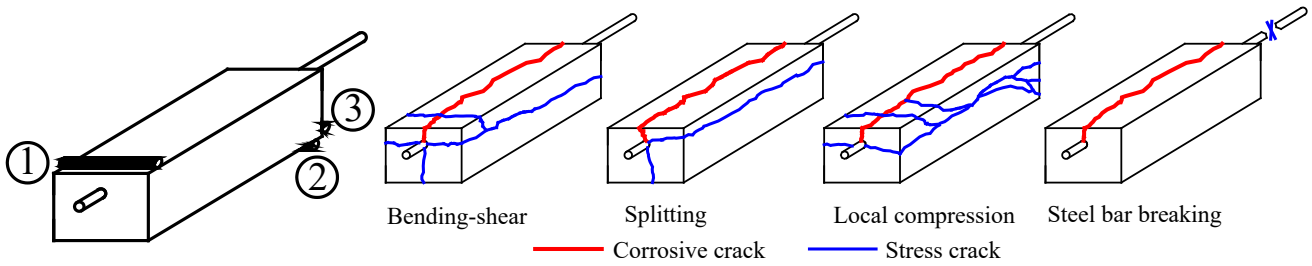

(a) Code of bearings (b) Failure modes

Figure 6. Types of damage

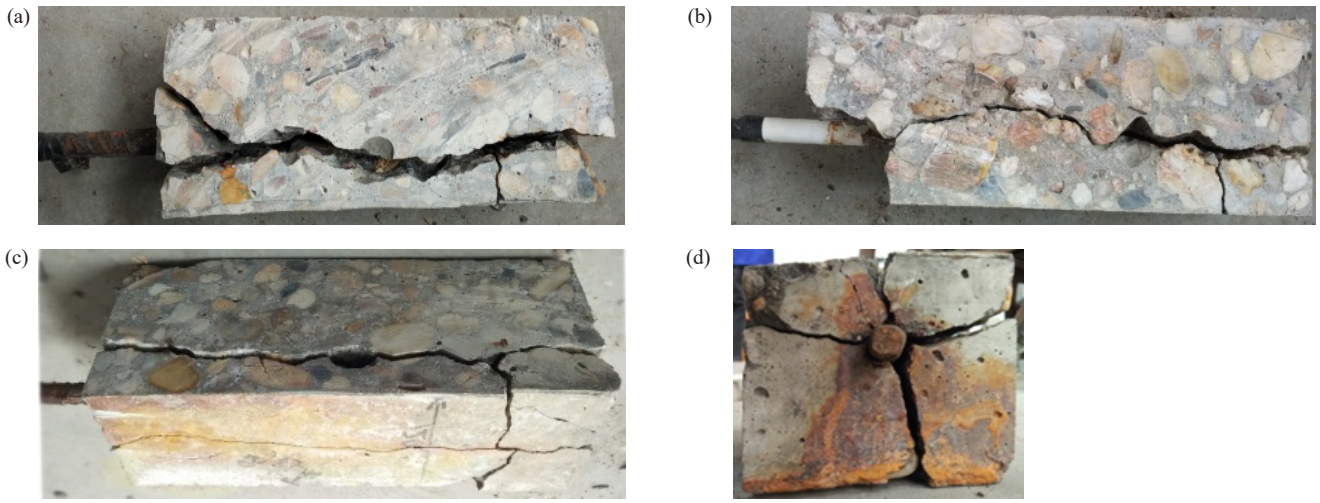

Figure 7. Bending-shear failure

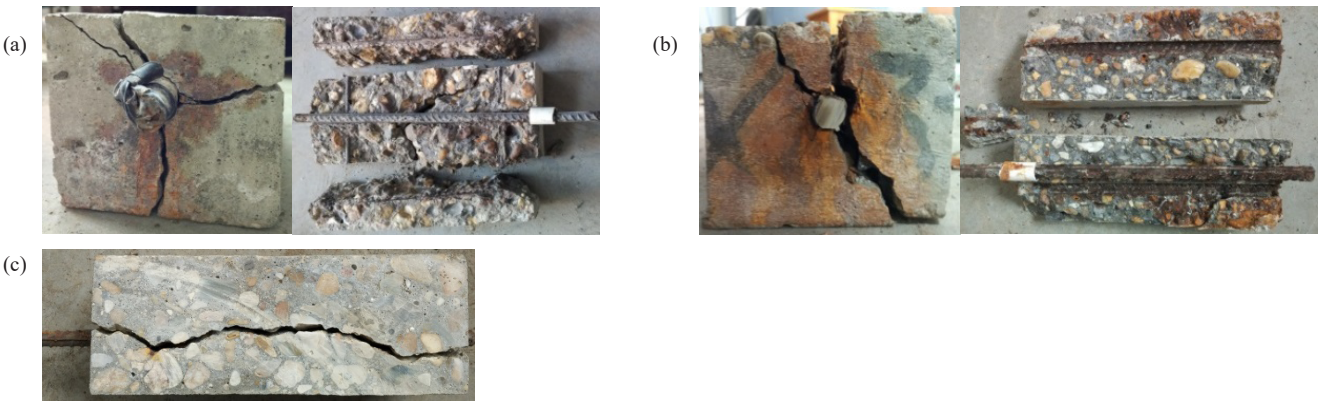

Figure 8. Splitting failure

Figure 9. Local compression failure

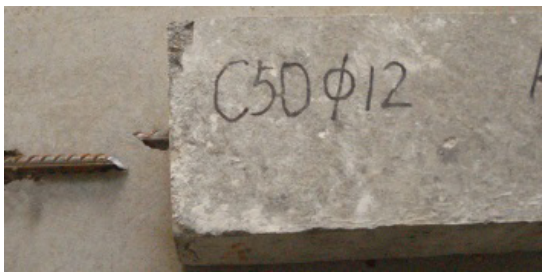

Figure 10. Steel bar breaking

Table 4. Test results

Code	Corrosion rate (%)	Maximum corrosive crack width (mm)	Average corrosive crack width (mm)	Load (kN)	Bonding strength (MPa)	$k_{\tau,u}$	Failure mode
N1-1C	0	0	0	56.5	5.995	1	Bending-shear
N1-1L3	4.5	0.22	0.145	57.5	6.101	1.0177	Splitting
N1-1L4	4.2	0.25	0.113	54.3	5.761	0.9610	Bending-shear
N1-1L5	6.4	0.78	0.302	50.0	5.305	0.8849	Bending-shear
N1-1M3	12.8	1.02	0.372	47.6	5.051	0.8425	Bending-shear
N1-1M4	12.1	1.11	0.433	28.0	2.971	0.4956	Splitting
N1-1M5	14.3	1.34	0.648	19.3	2.048	0.3416	Splitting
N1-1H3	19.7	2.00	1.260	7.8	0.828	0.1380	Splitting
N1-1H4	23.0	2.33	1.140	--	--	--	Damage
N1-1H5	26.5	2.40	1.030	--	--	--	Damage
N1-2C	0	0	0	77.0	7.003	1	Splitting
N1-2L3	2.3	0	0	78.6	7.148	1.0207	Bending-shear
N1-2L4	5.6	0.74	0.336	69.0	6.275	0.8960	Bending-shear
N1-2L5	4.0	0.52	0.270	72.1	6.557	0.9363	Splitting / local compression
N1-2M3	7.8	0.87	0.447	56.5	5.138	0.7337	Splitting
N1-2M4	10.5	1.32	0.638	45.2	4.111	0.5870	Splitting
N1-2M5	9.0	1.53	0.649	50.3	4.575	0.6533	Splitting

Table 1 (Continued)

Code	Corrosion rate (%)	Maximum corrosive crack width (mm)	Average corrosive crack width (mm)	Load (kN)	Bonding strength (MPa)	$k_{\tau,u}$	Failure mode
N1-2H3	11.7	1.21	0.705	34.9	3.174	0.4532	Splitting
N1-2H4	14.8	2.16	1.474	30.6	2.783	0.3974	Bending-shear
N1-2H5	13.3	1.85	1.330	33.6	3.056	0.4364	Splitting
N2-1C	0	0	0	71.6	7.597	1	Bending-shear
N2-1L3	2.0	0.07	0.031	78.9	8.372	1.1020	Steel bar breaking
N2-1L4	4.4	0.18	0.067	69.0	7.321	0.9637	Splitting
N2-1L5	4.8	0. 20	0.085	70.2	7.448	0.9804	Bending-shear
N2-1M3	7.5	0.87	0.429	68.2	7.236	0.9525	Splitting
N2-1M4	8.9	1.15	0.606	62.0	6.578	0.8659	Bending-shear
N2-1M5	9.4	1.07	0.644	63.1	6.695	0.8813	Bending-shear
N2-1H3	12.4	1.09	0.732	45.2	4.796	0.6313	Bending-shear
N2-1H4	13.6	1.28	1.210	30.2	3.204	0.4217	Splitting
N2-1H5	15.5	1.39	1.010	19.3	2.048	0.2696	Splitting
N2-2C	0	0	0	92.5	8.412	1	Splitting
N2-2L3	2.2	0	0	100.5	9.140	1.0865	Splitting
N2-2L4	4.3	0.26	0.195	95.8	8.713	1.0358	Bending-shear
N2-2L5	5.7	0.33	0.201	77.7	7.066	0.8400	Bending-shear
N2-2M3	6.7	0.73	0.401	67.4	6.130	0.7287	Splitting
N2-2M4	8.1	1.25	0.968	52.0	4.729	0.5622	Splitting
N2-2M5	7.8	0.88	0.542	59.6	5.420	0.6443	Splitting
N2-2H3	11.7	2.03	0.970	33.0	3.001	0.3568	Splitting
N2-2H4	12.9	2.15	1.240	35.6	3.238	0.3849	Splitting
N2-2H5	14.6	2.31	1.680	19.4	1.764	0.2097	Splitting

The average bonding stress between steel bar and concrete (referred to as "bonding stress") was calculated according to **Formula 1**. The bond-slip relationship curves of different series of specimens are shown in **Figure 11**. At the initial stage of loading, the slip amount (s) and the bond stress develop approximately linearly. With the increasing load, the growth rate of slip amount was accelerated, and the relation curve of the two was parabolic. The specimens with higher concrete strength grades required a greater load when the steel bars experienced significant slipping, and the slope of the rising section of the bond-slip curve was larger. The thickness of the protective layer of the specimens used in this test was c = 30 mm, and the slip amount of the steel bars in the specimens with larger nominal diameters was generally small. In the same series of specimens, with the increase in corrosion rate, the slope of the rising section of the bond-slip curve of the specimen was decreased, and a smaller load was required when the steel bar had an obvious slip.

$$\tau = \frac{N}{\pi dl} \quad (1)$$

Where N denoted the tensile force on the steel bar (N), d denoted the nominal diameter of the steel bar (mm), and l denoted bonding length (mm).

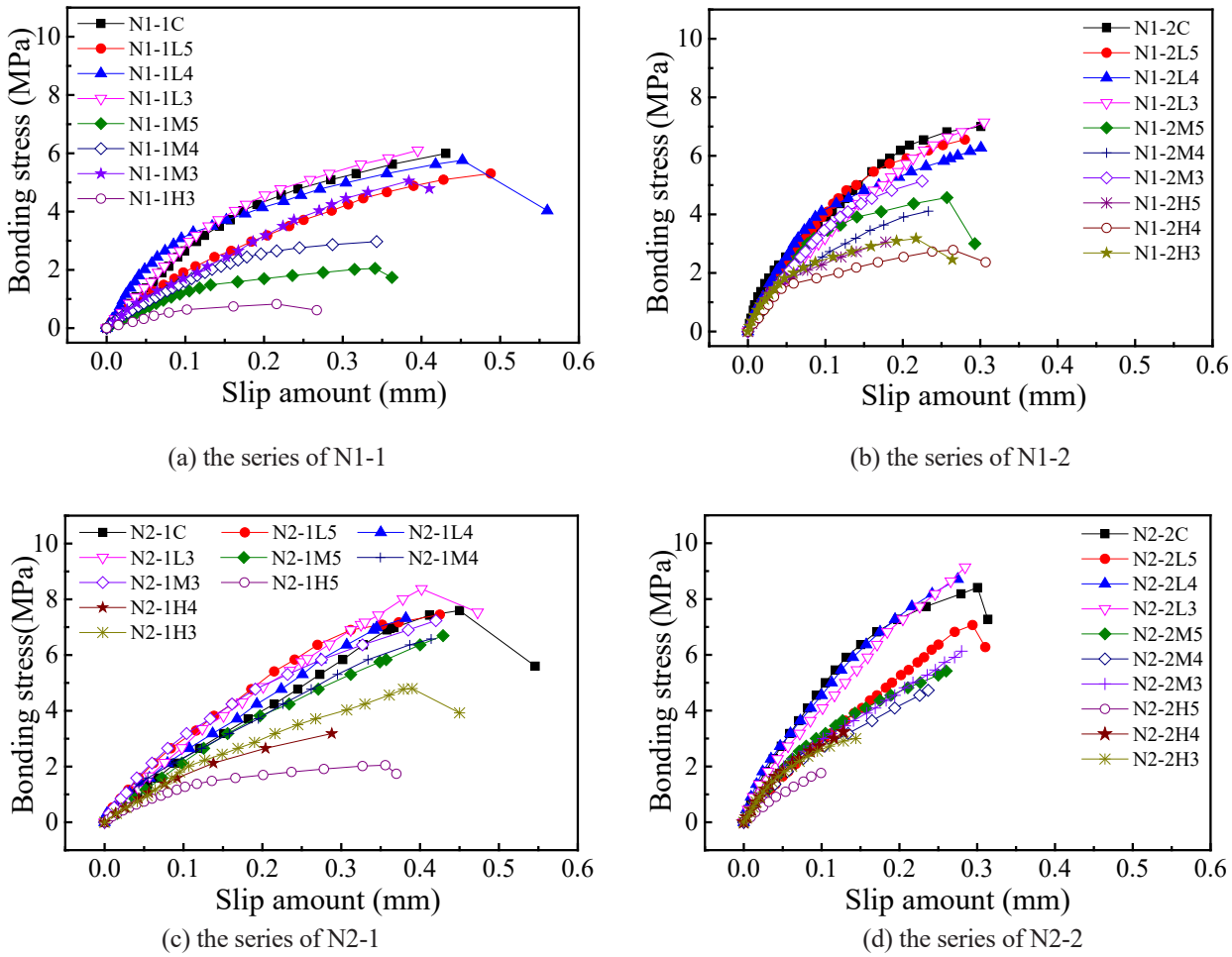

(a) the series of N1-1

(b) the series of N1-2

(c) the series of N2-1

(d) the series of N2-2

Figure 11. Bond-slip relationship curves

In general, none of the specimens in this experiment exhibited typical bond-slip failure. Upon reaching peak load, most specimens underwent brittle failure due to concrete cracking. A few specimens have the phenomenon of a plow scraping on the failure surface caused by steel bar sliding. Only specimen N2-1L3 experienced tensile failure of the steel bar. The mode of specimen failure was somewhat related to the width of corrosive cracks. When the corrosive cracks were wide, the specimens were prone to splitting along the existing corrosive cracks.

Figure 12 depicts the relationship between the ultimate bond strength τ_u and corrosion rates η for specimens of various series. The ultimate bond strength of specimens decreased with the increase in corrosion rate, and brittle splitting failure occurred more often. Specimens with high concrete strength generally had slightly higher bond strength values. When $\eta < 5\%$, the ultimate bond strength of the specimen was significantly increased compared with that uncorroded. However, the rate of decrease in ultimate bonding strength was also greater when the corrosion rate increased.

The ratio of the thickness of the protective layer to the diameter of the steel bar c/d was 2.5 (the series of N1-1 and N2-1) and 2.14 (the series of N1-2 and N2-2), respectively. When $\eta < 5\%$, specimens with smaller c/d have more corrosion products per unit surface area of steel bars, and the concrete did not show obvious cracking. Therefore, the restraint force caused by the corrosion expansion enhances the bonding ability between steel bars and concrete. However, with the increase in corrosion rate, the rib pattern on the surface of the steel bar was lost, the concrete cracked severely, and the bond strength between the steel bar and concrete decreased

rapidly. These phenomena were most evident in the series of N2-2 specimens.

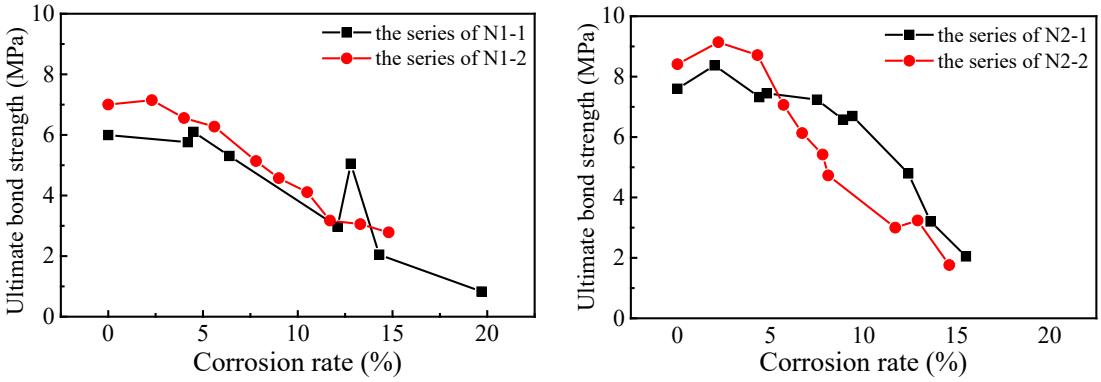

Figure 12. The relationship between Bonding Strength and corrosion rate

4. Bonding performance

4.1. Degradation of bonding strength

A parameter $k_{\tau,u}$ is defined as the relative ultimate bonding strength. The calculation method is shown in **Formula 2**, which takes the ratio of the ultimate bonding strength of corroded specimens to the ultimate bonding strength of non-corroded specimens of the same series.

$$k_{\tau,u} = \frac{\tau_{\mathrm{C,u}}}{\tau_{\mathrm{N,u}}} \qquad (2)$$

Where $\tau_{C,u}$ denoted the ultimate bonding strength of corroded specimen (MPa), $\tau_{N,u}$ denoted the ultimate bonding strength of uncorroded specimen (MPa).

The experimental results show that when the corrosion rate is low, the effect of steel bar corrosion on the bonding strength of the specimens is not significant, and the bonding strength of some specimens has improved slightly. When the corrosion rate was low, the specimen did not crack or only cracked slightly, and the corrosion products would fill the gap between the steel bar and concrete, which helped improve the bonding strength. The bonding strength between the steel bar and the concrete gradually decreased as the corrosion rate further increased, attributed to the widening of corrosive cracks and loss of surface ribs on the steel bar due to corrosion. Through regression analysis, the relationship between the relative ultimate bond strength of the specimen and the corrosion rate is obtained as shown in **Figure 13**. The calculation method of bonding strength is shown in Equation 3. To simplify the calculation, $k_{\tau,u}$ of the specimen whose corrosion rate did not exceed 2.6% was set to 1.0, which would make the calculation results more accurate.

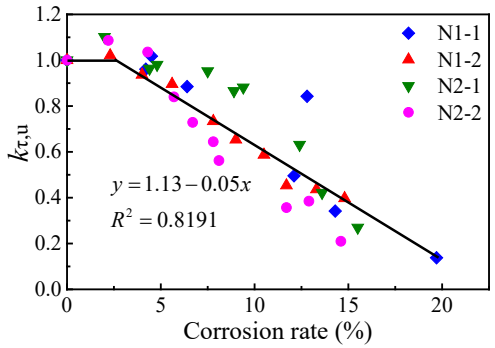

Figure 13. The relationship between relative ultimate bonding strength and corrosion rate

$$k_{\tau,u} = \frac{\tau_{N,u}}{\tau_{C,u}} = \begin{cases} 1.0 & \eta \le 2.6\% \\ 1.13\text{-}0.05\eta & \eta > 2.6\% \end{cases} \quad (3)$$

The corrosive crack is an intuitive reflection of the corrosion degree of the component, and the width of the corrosive crack is easy to measure. Therefore, from a practical engineering perspective, using the relationship between the width of corrosive cracks and the bonding performance of corroded reinforced concrete components is more operable for evaluating the decrease in bonding strength caused by corrosion. There are two solutions to this problem: the first one is to establish the relationship between the width of corrosive cracks in components and the corrosion rate of steel bars and then predict the decrease in bonding force of components through the corrosion rate. Many domestic and foreign studies have adopted this method and obtained good results. Another approach is to directly establish the relationship between the width of corrosive cracks and the bonding strength of components. Al-Sulaimani *et al.* [21] and Law *et al.* [22,23] provided a mathematical relationship between the surface crack width of the component and the degradation of bonding force based on beam end tests of accelerated corrosion specimens, respectively. Tahershamsi *et al.* [24,25] investigated the relationship between corrosive crack width and anchorage bearing capacity through naturally corroded beam components. They also pointed out that based on the model obtained from accelerated corrosion tests, using the width of corrosive cracks as an evaluation indicator may make the evaluation results biased toward safety. Some regulations in Europe provide a rough relationship between the width of corrosive cracks on the surface of components and the bonding strength. The range of changes in the corresponding bonding strength can be calculated by the range of changes in the width of corrosive cracks [26]. However, in general, the relevant research using the second approach is still relatively limited, and further experimental research and analysis are needed.

Figures 14 & 15 show the relationship between the relative ultimate bonding strength of the specimen and the ultimate and average corrosive crack width, respectively. Through regression analysis, it can be found that there is a highly consistent linear variation pattern between the relative ultimate bonding strength of the specimen and the width of the corrosive crack (Equations 4 and 5).

$$k_{\tau,u} = 1 - 0.322\omega_C \quad (4)$$

$$k_{\tau,u} = 1 - 0.522\omega_m \quad (5)$$

where ω_c denoted the ultimate width of corrosive crack (mm); ω_m denoted the average width of corrosive crack (mm).

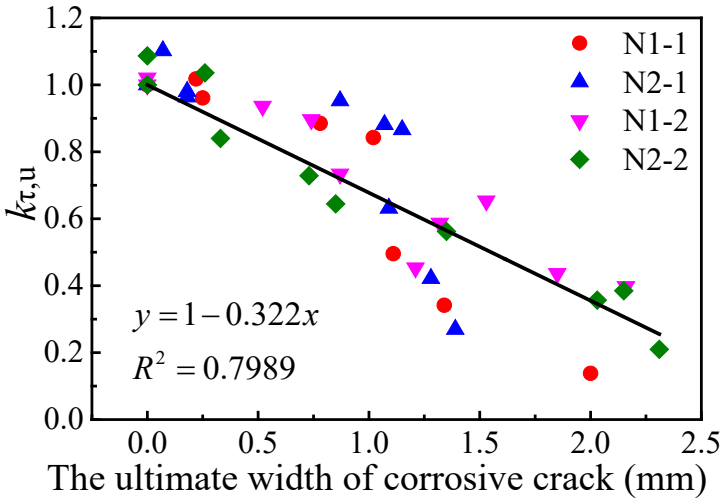

Figure 14. $k_{\tau,u} - \omega_c$

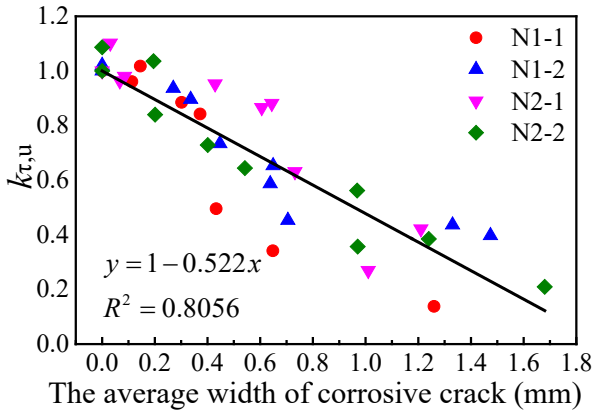

Figure 15. $k_{\tau,u} - \omega_m$

4.2. Bond-slip constitutive relation

This experimental study focuses on plate components with weak lateral constraints, mainly considering the influence of corrosion degree on bonding performance. It attempts to obtain a continuous bond-slip constitutive model of corroded reinforced concrete components through regression analysis. The bonding stress and slip amount of the test specimens were normalized: the bonding stress τ was divided by the peak bonding stress $\tau_{N,u}$ of the same series of uncorroded specimens to obtain the relative bonding stress k_τ (Equation 6); the slip amount (s) was divided by the peak slip amount $s_{N,u}$ (The slip amount corresponding to the peak bonding stress) to obtain the relative slip amount k_s (Equation 7).

$$k_\tau = \frac{\tau}{\tau_{N,u}} \tag{6}$$

$$k_s = \frac{s}{s_{N,u}} \tag{7}$$

The bond-slip constitutive relationship of corroded steel reinforcement components is shown in Equation 8 and **Figure 16**. The model takes the (mass) corrosion rate (η) as the main control index. The model is in good agreement with the test when the corrosion rate of specimens did not exceed 28% and mainly experienced splitting failure ($R^2 = 0.9377$).

$$k_\tau = (-2.216k_s^4 + 5.032k_s^3 - 4.543k_s^2 + 2.798k_s) \times (1 - 3.595\eta) \tag{8}$$

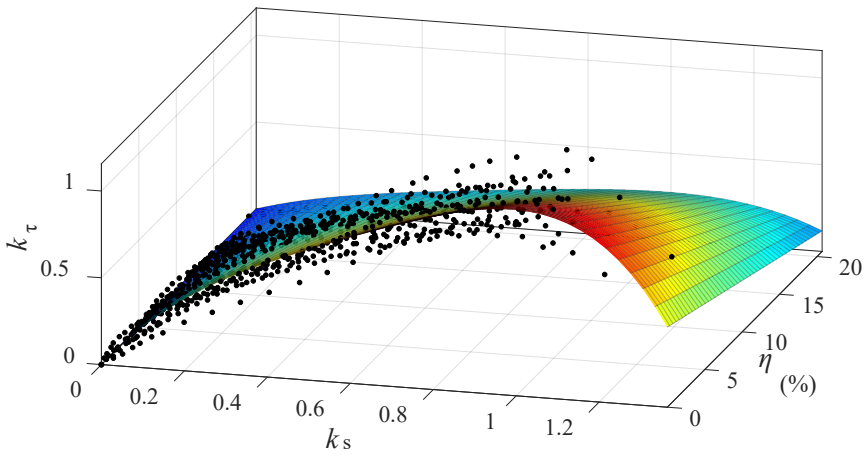

Figure 16. Bond-slip constitutive model

5. Conclusion

This study focuses on the degradation of bonding performance of corroded steel bars in slab components with weak lateral constraints. The bond-slip curve was obtained through a half-beam test, and the changes in the bonding performance of HRB500E and HRB400 steel bar specimens with different degrees of corrosion were compared and analyzed. Formulas for calculating the ultimate bonding strength were established using the mass corrosion rate of steel bars and the width of corrosive cracks in specimens as control variables, and a continuous bond-slip constitutive model was regressed based on the experiments.

(1) Specimens with lower corrosion rates and smaller width of corrosive cracks mainly exhibited bending shear failure, while specimens with higher corrosion rates and wider corrosive cracks mainly exhibited splitting failure.

(2) The ultimate bonding strength of corroded reinforced concrete specimens shows an overall decreasing trend with the increase of corrosion rate. When $\eta < 5\%$ the ultimate bonding strength of specimens with higher concrete strength was increased compared to those uncorroded. However, as the corrosion rate increases, the rate of decrease in the ultimate bonding strength is also greater.

(3) The relationship between the relative ultimate bonding strength, the corrosion rate of steel bars, and the width of corrosive cracks was obtained through experiments. There was a linear pattern between the increase of corrosive crack width and the decrease of bonding force in components, which could provide a basis for evaluating the degree of bonding strength reduction of corroded components in practical engineering.

(4) The bond-slip constitutive relationship between corroded steel bars and concrete was established by using relative bond stress and relative slip amount, which is in good agreement with the experimental results.

Funding

Scientific Research Fund of Hunan Provincial Education Department (21A0123)

Disclosure statement

The authors declare no conflict of interest.

References

[1] Liang X, He F, Li X, et al., 2022, Research Progress on Strength and Bond Properties of Corroded Steel Bars. Building Structure, 52(S1): 1571–1575.

[2] Zhuang B, Xiao C, Liu Q, et al., 2022, Experimental Study on Bond-Slip Mechanical Properties of Concrete with Different Admixtures and Corroded Reinforcement. Bulletin of the Chinese Ceramic Society, 41(8): 2767–2773.

[3] Wang C, Wu Y, Chao F, et al., 2022, Experimental Study on Bond Behavior Under Coupling Effect of Freezing-Thawing Between Corroded Steel Bar and Recycled Concrete. Journal of Building Structure, 43(Suppl.1): 382–393.

[4] Alsulaimani GJ, Kaleemullah M, Basunbul IA, 1990, Influence of Corrosion and Cracking on Bond Behaviour and Strength of Reinforced Concrete Members. ACI Structural Journal, 87(2): 220–231.

[5] Rodriguez J, Ortega LM, Casal J, et al., 1994, Corrosion of Reinforcement and Service Life of Concrete Structures: Corrosion and Bond Deterioration. International Conference on Concrete Across Borders, 315–326.

[6] Almusallam AA, Al-gahtani AS, Aziz AR, et al., 1996, Effect of Reinforcement Corrosion on Bond Strength. Construction and Building Materials, 10(2): 123–129.

[7] Stanish K, Hooton RD, Pantazopoulou SJ, 1999, Corrosion Effects on Bond Strength in Reinforced Concrete. ACI Structural Journal, 96(6): 915–921.

[8] Mangat P, Elgarf M., 1999, Bond Characteristics of Corroding Reinforcement in Concrete Beams. Materials and Structures, 32(2): 89–97.

[9] Yuan Y, Yu S, Jia F, 1999, Deterioration of Bond Behavior of Corroded Reinforced Concrete. Industrial Construction, 29(11): 47–50.

[10] Eligehausen R, Popov EP, Bertero VV, 1983, Local Bond Stress-Slip Relationships of Deformed Bars Under Generalized Excitations, dissertation, University of California, 69–80.

[11] Ciampi V, Eligehausen R, Bertero V V, et al., 1981, Analytical Model for Deformed Bar Bond Under Generalized Excitations. Trams IABSE Colloquium on Advanced Mechanics of Reinforced, 53–67.

[12] Xu Y, Wang H, Shi Z, 1990, Experimental Study on Bond-Anchorage Mechanism of Steel Bar. Proceedings of the Second Symposium on Basic Theory and Application of Concrete Structures (volume I), 211–218.

[13] Somayaji S, Shan SP, 1981, Bond Stress Versus Slip Relationship and Cracking Response of Tension Members. ACI, Journal Proceedings. 78(3): 217–225.

[14] Zhao Y, Jin W, 2002, Test Study on Bond Stress-Slip Relationship of Concrete and Steel Bar. Journal of Building Structure, 23(1): 32–37.

[15] Wu YF, Zhao XM., 2014, Unified Bond Stress-Slip Model for Reinforced Concrete. Journal of Structural Engineering, 139(11): 1951–1962.

[16] Nilson AH, 1972, Internal Measurement of Bond Slip. ACI Journal Proceedings, 69(7): 439–441.

[17] Yuan Y, Jia F, Cai Y, 2001, The Structural Behavior Deterioration Model for Corroded Reinforced Concrete. China Civil Engineering Journal, 34(3): 47–52.

[18] Zhang W, Zhuang Y, 2001, Study on the Constitutive Relationship of Bond Slip Between Corroded Reinforcement and Concrete After Cracking. China Civil Engineering Journal, 34(5): 40–44.

[19] Kivell A, Palermo A, Scott A, 2015, Complete Model of Corrosion-Degraded Cyclic Bond Performance in Reinforced Concrete. Journal of Structural Engineering, 141(9): 04014222.

[20] Fang L, 2021, The Research on Flexural Behavior of Corroded HRB500 Reinforced Concrete Members, thesis, College of Civil Engineering, dissertation, Hunan University, 25–50.

[21] Al-Sulaimani GJ, Kaleemullah M, Basunbul IA, et al., 1990, Influence of Corrosion and Cracking on Bond Behavior and Strength of Reinforced Concrete Members. ACI Structural Journal, 87(2): 220–231.

[22] Law DW, Tang D, Molyneaux TKC, et al., 2011, Impact of Crack Width on Bond: Confined and Unconfined Rebar. Materials and Structures, 44(7): 1287–1296.

[23] Tang D, Molyneaux TK, Law DW, et al., 2011, Influence of Surface Crack Width on Bond Strength of Reinforced Concrete. ACI Materials Journal, 108(1): 29–37.

[24] Tahershamsi M, Fernandez I, Lundgren K, et al., 2016, Investigation Correlations Between Crack Width, Corrosion Level and Anchorage Capacity. Structure and Infrastructure Engineering, 13(10): 1294–1307.

[25] Lundgren K, Tahershamsi M, Zandi K, et al., 2015, Tests on Anchorage of Naturally Corroded Reinforcement in Concrete. Materials and Structures, 48(7): 2009–2022.

[26] Lin H, 2017, Experimental Study on the Bond Behavior of Corroded Reinforced Concrete under Monotonic or Repeated Loading, thesis, College of Civil Engineering and Architecture, Zhejiang University, 1–29.